Reexamination of the Lyman-Birge-Hopfield transition of N_2: Configuration-interaction generalized oscillator strengths

Tiago Giannerini
Centro Federal de Educação Tecnológica de Química de Nilópolis, Rua Lúcio Tavares, 1045, Nilópolis, 26530-060, Rio de Janeiro, Brazil

Itamar Borges, Jr.
Departamento de Química, Instituto Militar de Engenharia, Praça General Tibúrcio, 80, Rio de Janeiro 22590-270, Rio de Janeiro, Brazil

Eduardo Hollauer
Departamento de Físico-Química, Instituto de Química, Universidade Federal Fluminense, S-N Valonguinho, Niterói, Rio de Janeiro 24020150, Brazil

(Received 19 July 2006; revised manuscript received 3 November 2006; published 9 January 2007)

Generalized oscillator strengths (GOS) for the dipole forbidden quadrupole allowed Lyman-Birge-Hopfield (LBH) valence transition of N_2 have been calculated. Complete active space self-consistent-field (CAS) and multireference configuration interaction (MRCI) wave functions of several types have been used and their effects on the computed GOS profiles discussed. Orthogonal and nonorthogonal molecular orbitals have been employed. The latter allows the explicit inclusion of relaxation effects in the excited state leading to a clear spectra interpretation. Hartree-Fock (HF) and CAS wave functions have been compared as a previous step before the MRCI calculations. Differences between the respective GOS profiles were found, with the CAS MRCI GOS curve being slightly closer to experiment than the HF MRCI one. Agreement between the present theoretical CAS MRCI GOS profile employing nonorthogonal orbitals and recent experimental results are very favorable, being the best one among available theoretical calculations in the literature.

DOI: 10.1103/PhysRevA.75.012706 PACS number(s): 34.80.Gs, 31.15.Ar

I. INTRODUCTION

Measurements and calculations of generalized oscillator strengths (GOS), a quantity proportional to high energy electron impact differential cross sections, provide information of major importance for discrete and continuum molecular spectra interpretation [1–6]. GOS profiles, which are experimentally derived from electron impact spectroscopy instead of photon absorption, allow dipole forbidden electronic transitions, in addition to dipole allowed ones, to be measured and studied. In particular, the molecular nitrogen, which is a major component of the earth atmosphere, has an important valence dipole forbidden transition at 9.3 eV. This quadrupole allowed transition, called the Lyman-Birge-Hopfield (LBH) band, corresponds to the $X\ ^1\Sigma_g^+ \rightarrow a\ ^1\Pi_g$ transition and is considered according to Leung as "one of the classic benchmark molecular systems for absolute GOS measurements today" [5].

Experimental measurements of the LBH GOS were first made in the pioneer Lassetre group [7]. Other measurements followed [8–12] including the 1999 result of Leung [5]. Concerning the theoretical side, there are only three works on this band, namely, the Tamn-Dancoff (TDA) and random phase (RPA) approximations of Szabo and Ostlund [13], the Hartree-Fock of Chung and Lin [14] and the Hartree-Fock configuration interaction of Ref. [1]. Szabo and Ostlund used a minimal basis set of Slate-type orbitals and Chung and Lin employed several small basis sets eventually including polarization functions. As these theoretical GOS results were obtained at insufficient levels of theory, they will not be further discussed. An early work [1] used a hand-made $(12s,7p,1d)/[9s,5p,1d]$ Gaussian basis set that started from an old Dunning double-ζ basis set and added s and p diffuse functions and a d-polarization function. As far as the authors are concerned, Ref. [1] is the most recent calculation on this transition. The three theoretical works described the electron scattering through the first Born approximation.

A more efficient computer code for GOS calculations through the first Born approximation was developed and used to study the LBH band in the present work. The program allows the possibility of including the effect of direct relaxation of excited orbitals as opposed to the frozen-core approximation usually employed [13,14]. In order to obtain more accurate theoretical GOS profiles of this band, make comparisons with more recent experimental results [5] and to further test our developed code, we revisit theoretically the Lyman-Birge Hopfield band. We have used Hartree-Fock or complete active space self-consistent-field (CAS) followed by multireference configuration interaction (MRCI) wave functions of several types as well as orthogonal and nonorthogonal molecular orbitals. The effect of the wave function and relaxation degree in the GOS results is discussed.

II. THEORETICAL FRAMEWORK

The GOS f_{on} for the transition between the 0 and n states, in the first Born approximation is given by the following expression [15]:

$$f_{on}(K) = \frac{2\Delta E g_n}{K^2} \int \frac{d\Omega}{4\pi} \left| \langle \Psi_n | \sum_{j=1}^{N} e^{i\mathbf{K}\cdot\mathbf{r}_j} | \Psi_0 \rangle \right|^2,$$

where $\mathbf{K}$ is the transferred momentum and equals $\mathbf{k}_0 - \mathbf{k}_n$, $\mathbf{k}_0$ and $\mathbf{k}_n$ are the momenta of the incident and scattered electron, respectively. The degeneracy of the final state is represented by g_n, being 2 for a Π state and ΔE is the transition energy. The summation is over the N electrons in the target molecule localized by the corresponding $\mathbf{r}_j$ vector. The electronic wave functions for the initial (0) and final (n) states are given by Ψ_0 and Ψ_n. A summation over all the final vibrational levels is implied. Therefore, the reported f_{on} values correspond to the whole band. The integration over Ω results from averaging over the orientation of the molecular axis with respect to $\mathbf{K}$, i.e., the classical average.

Several configuration interaction wave functions were used to describe both electronic states. Multireference CI (MRCI) wave functions were generated from a reference space constructed from a previous CI singles and doubles (CISD) calculation including only configurations from the latter with CI coefficients over 0.1. The active space consisted of the first 13 virtual orbitals in this way making up 20 orbitals. The other CI wave functions included a previous CAS calculation before the CI step. The CAS calculation included the full valence space of N_2 (FVCAS). The CAS MRCI employed as reference space CAS configurations having coefficients over 0.1. For the largest basis set used, the $(12s,7p,1d)/[9s,5p,1d]$ set [1], about 33 000 configurations were generated for each state. A larger active space was also employed—see below. In the GOS computations including relaxation of the orbitals, a separate FVCAS was done for each state. In the froze-core approximation, where the same CAS wave functions were used for both states, state averaged orbitals provided a balanced set of molecular orbitals for the CI wave function [16,17]. Therefore, GOS calculations employed HF CISD, HF MRCI, CAS CISD, and CAS MRCI wave functions expanded on contracted Gaussian basis sets.

Three different Gaussian basis sets have been used. A previously used $(12s,7p,1d)/[9s,5p,1d]$ [1], the aug-*cc*-*p*VDZ basis set and a triple-zeta *cc*-*p*VTZ excluding the f function [18], thereafter called *cc*-*p*VTZ′. The reason for the exclusion of the f function is that this angular momentum has not yet been implemented in our code. The basis sets size was determined by our computer limitations. All calculations were carried out at the N_2 equilibrium distance of $2.068a_0$.

Two different approaches for the molecular orbital set were employed to describe the LBH transition. In the first one, both ground and excited states were described from the same set of orthogonal orbitals, optimized for the molecular ground state, the so-called frozen-core approximation. Virtual orbitals were obtained according to the modified virtual orbitals (MVO) technique [19] with the removal of two electrons. This approach improves the excited character of the virtual orbitals, being specially important for orthogonal calculations. In the second type of molecular orbitals used to build the wave functions for the GOS calculations, the orbitals of each state were independently converged for each electronic state. In this case the virtual orbitals were not modified. Therefore, a complete relaxation of the excited state molecular orbitals was achieved—this is the nonorthogonal case.

The classical, or rotational average, in the first Born approximation framework, is carried out through a transition density matrix generated for the CI wave function of both states, using orthogonal or nonorthogonal orbitals. This approach is particularly important since it is possible to compute the GOS for a large number of transferred momenta values without great computational demand. Since the rotational integral is done numerically, we did test calculations to obtain the optimum size of the two-dimensional grid (i.e., number of points along each angle). HF CISD wave functions, nonorthogonal orbitals and the largest basis set were employed for this test. Let us define a pair of numbers, the first to represent the Θ integration and the second the Φ one. After running GOS test calculations we reached the conclusion that the (28,58) grid is sufficient to obtain an equivalent accuracy when compared with larger grids and at the same computational cost. In order to illustrate this point: the (28,58) grid takes 29.90 minutes and contains 1624 points for a GOS calculation while the (97,199) grid, with 298.75 min and 19 303 points, presents results of similar accuracy.

All calculations employed a 933 MHz computer with 256 Mb of RAM. The electronic HF and CAS wave functions were obtained with the GAMESS-US program while for the CI wave functions a program developed by Hollauer and co-workers was used.

III. RESULTS AND DISCUSSION

A. Basis sets effects

First, we discuss the effect of the type of basis set and wave functions on frozen-core (orthogonal) and relaxed (nonorthogonal) computations of GOS. The GOS calculations employed the following wave functions: CAS, CAS CISD*, CAS CISD, CAS MRCI*, and CAS MRCI. All the CI calculations used the full set of orbitals generated by the corresponding Gaussian basis set except the ones that have the label*. In such cases, the CI wave funtions were constructed from a reduced active space composed of the first 20 orbitals. The basis set $(12s,7p,1d)/[9s,5p,1d]$ has a total of 60 functions while the other two sets have 50.

For the orthogonal CAS wave functions using the three basis sets the GOS results are essentially indistinguishable showing a maximum at $K^2 \sim 1.0$ a.u. However, the picture changes when a CISD wave function is obtained from the CAS. While the $(12s,7p,1d)/[9s,5p,1d]$//CAS CISD* results have the maximum at $\sim$1.0 a.u. the other basis sets have them at $\sim$0.8 a.u.; for greater values of K^2 the $(12s,7p,1d)/[9s,5p,1d]$//CAS CISD* calculation presents the lower values. When all orbitals are included in the CI calculation, the curves' pattern is more well behaved, with the calculated GOS showing descending values in the following basis set order: $(12s,7p,1d)/[9s,5p,1d]$,

TABLE I. Comparison between computed transition energies using different basis sets, orthogonal and nonorthogonal orbitals, wavefunctions and experimental data. Table values reported in electron-volts (eV).

	$(12s,7p,1d)/[9s,5p,1d]$		aug-cc-pVDZ		cc-pVTZ′	
Level	Orthogonal	Nonorthogonal	Orthogonal	Nonorthogonal	Orthogonal	Nonorthogonal
CAS	10.32	10.17	10.32	10.18	10.37	10.24
CAS/CISD(R)	10.24	10.41	10.14	10.27	9.98	10.01
CAS/CISD	9.83	9.78	9.75	9.73	9.79	9.77
CAS/MRCI(R)	10.19	10.34	10.04	10.20	9.80	9.84
CAS/MRCI	9.71	9.70	9.62	9.62	9.68	9.48
Experimental						
Lucas [10]	9.2					
Fainelli [11]	9.32					
Barbieri [12]	9.35					
Leung [5]	9.3					

aug-cc-pVDZ, cc-pVTZ′ and coinciding for large K^2 values. The behavior of the GOS for the CAS MRCI wave functions with reduced and complete active spaces is similar to the CAS CISD calculations involving the same active spaces, so the previous discussion applies here. These theoretical GOS values are close to the experimental values [5,10] except at the maximum regions where theory overestimate experiment, especially the $(12s,7p,1d)/[9s,5p,1d]$ results.

For nonorthogonal calculations the overall behavior is similar to the orthogonal computations. The noticeable differences are (i) for the CAS calculation the maximum region is slightly dislocated to the left; (ii) the CISD and MRCI calculations with reduced active space are similar to the previous orthogonal results, but in the former the difference among the results is lower, being almost inexistent between aug-cc-pVDZ and cc-pVTZ′ basis sets; this shows that inclusion of relaxation improves the convergence for the three basis sets; (iii) The CAS CISD GOS, that includes the complete active space and nonorthogonal orbitals, present a similar pattern compared with the orthogonal results, but the difference among them is lower; (iv) the results at the highest level, CAS MRCI, show the same overall behavior of the orthogonal results, however the agreement among them is not present at the maximum region, although the ordering as function of the basis set is maintained.

Some conclusions can be drawn from the above analysis. While the CAS calculations do not differentiate the basis set quality, the CAS CISD and CAS MRCI GOS show distinct results for each one, especially at the maximum region. It is interesting to note that although the $(12s,7p,1d)/[9s,5p,1d]$ basis set is the largest, the results with the correlation consistent basis sets are closer to the experimental results (see later). This might indicate the more balanced character and appropriateness of the correlation consistent basis set than "hand-made ones." This approach could allow in the future basis-set extrapolation of the GOS, as was done before for optical oscillator strengths [17,20]. The sequence of wave functions just presented may be thought of as an hierarchical sequence of wave functions, as the clear cut one existing for coupled-cluster wave functions [17,21].

B. Transition energies

One measure of the quality and balancing of the theoretical description of ground and excited states, and of properties computed from them, is the vertical transition energy. Although the comparison with experimental data should be viewed with caution [22], especially for polyatomics, it is still illuminating and will be carried out in the following.

In Table I the computed transitions energies for the Lyman-Birge-Hopfield band are presented along available experimental values. All calculations presented transition energies higher than the measured values. The computed values decrease with the increase of wave-function quality (i.e, the correlation level). The CAS wave functions have transition energies over 10 eV, with the use of nonorthogonal values reducing them ~0.14eV. The CISD and MRCI calculations employing the reduced active space (* label) presented also transition energies over 10 eV, the exception being for the cc-pVTZ′ basis set. The best agreement with the experimental values comes from the wave functions including all generated orbitals, namely, CAS CISD and CAS MRCI. It may be noticed that the transition energies for these wavefunctions showed similar values for the aug-cc-pVDZ and cc-pVTZ′ basis sets. The computed transition energy showing the best agreement with experiment used the cc-pVTZ′//CAS MRCI method with nonorthogonal orbitals. This value showed a difference of less than 2% when compared with the experimental average. A lowering of 0.20 eV was obtained with the nonorthogonal orbitals, a patent manifestation of the importance of relaxation effects even in a valence transition. The best calculation available until now, the HF CI calculations by Hollauer and co-workers including up to quadruple excitations and nonorthogonal orbitals [1], obtained 9.80 eV for the transition energy, a result worse than ours.

The computed transition energies show similar trends of the GOS calculations: the values get closer to the experimental values with the inclusion of more electronic correlation through higher quality wave functions. This hierarchy of wave functions is identical to the one discussed in the preceding section for the GOS. Similarly, one could establish the following sequence of basis set quality: $(12s,7p,1d)/[9s,5p,1d]$, aug-*cc*-pVDZ and *cc*-*p*VTZ′. It should be stressed that this basis set sequence does not follow the number of basis functions of each set, and might be an indication of the inadequacy of basis set "hand-made" construction for high accuracy computation of transition properties.

C. Relaxation effects

In order to systematically investigate relaxation effects, GOS calculations were carried out with the three basis sets employing orthogonal (i.e., frozen core approximation) and nonorthogonal orbitals.

With the exception of the CAS GOS, the other GOS computations employing the CAS CISD*, CAS CISD, CAS MRCI*, and CAS MRCI wave fuctions and the *cc*-*p*VTZ′ basis set present orthogonal and nonorthogonal results essentially coincident. The differences between orthogonal and nonorthogonal CAS GOS values seem to indicate that the CAS orbitals optimized for the ground state are not capable of describing the relaxation effects occurring in the excited states. A similar trend was observed in the optical oscillator strengths computations of a valence-Rydberg transition in water [17]. Concerning these GOS calculations, the same wave functions and the other two basis sets, some comments are in order. The GOS results employing the CAS CISD*, and the CAS MRCI*, wave functions, which did not use the whole set of molecular orbitals (i.e., using a restricted active space), for the $(12s,7p,1d)/[9s,5p,1d]$ and aug-*cc*-*p*VDZ basis sets, do not show coincident GOS curves. This fact may be an indication of insufficient correlation recovery for GOS calculations with the $(12s,7p,1d)/[9s,5p,1d]$ and aug-*cc*-*p*VDZ basis sets combined with CAS CISD* and CAS MRCI* wave functions and orthogonal and nonorthogonal orbitals. This is the opposite situation of the GOS results using the *cc*-*p*VTZ′ basis set and the same wave functions.

The situation just presented indicates that the *cc*-*p*VTZ′ basis set is the most adequate for GOS calculations of this valence transition. This will be further considered when we compare our results with experimental GOS data.

D. Correlation effects and comparison with previous theoretical and experimental results

The importance of correlation effects is well known for the calculation of ground state properties, but these effects are especially critical when excited states are involved. In Fig. 1 we present the results of GOS calculations employing the wave functions above described, the *cc*-*p*VTZ′ basis set with orthogonal (a) and nonorthogonal (b) orbitals.

Concerning a hierarchical sequence of wave functions in order of increasing accuracy (i.e., approaching the experimental data), the GOS behavior for orthogonal and nonorthogonal follows the order: CAS, CAS CISD* CAS MRCI*, CAS CISD, and CAS MRCI. It is worth noticing that the separation between the CAS CISD and CAS MRCI GOS curves is more pronounced for relaxed orbitals.

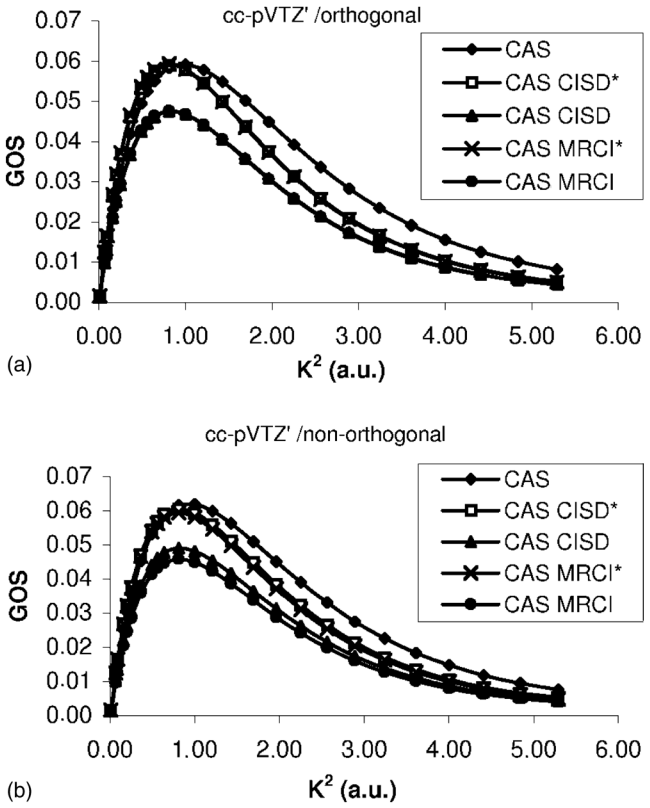

FIG. 1. Calculated GOS profiles at different correlation levels (i.e., wave functions) using (a) orthogonal and (b) nonorthogonal orbitals.

An important, though unexplored question, arises when GOS results computed with HF, CAS, HF MRCI, and CAS MRCI wave functions are compared [20]. This comparison could establish, concerning the GOS for the LBH transition, if there is any difference on the computed results depending on the use of CAS wave functions, which also optimizes molecular orbitals, or Hartree-Fock ones, which do not optimize them. We have done that using the $(12s,7p,1d)/[9s,5p,1d]$ basis set and orthogonal orbitals. The major differences are between HF MRCI* and CAS MRCI* GOS curves, which employ a smaller reference CI space than in the HF MRCI and CAS MRCI curves. The latter wave functions present very close GOS curves and are the closest to the experimental data (see below). It is interesting to notice that the GOS curves using the CI singles and doubles (CISD) wave function are indistinguishable whether the previous step employs Hartree-Fock or CAS orbitals, although the HF MRCI and CAS MRCI results are closer to experiment, as will be discussed later.

In Fig. 2 we compare our GOS CAS MRCI//*cc*-*p*VTZ′ calculations employing nonorthogonal orbitals (full curve), our most accurate one, with the previous theoretical and ex-

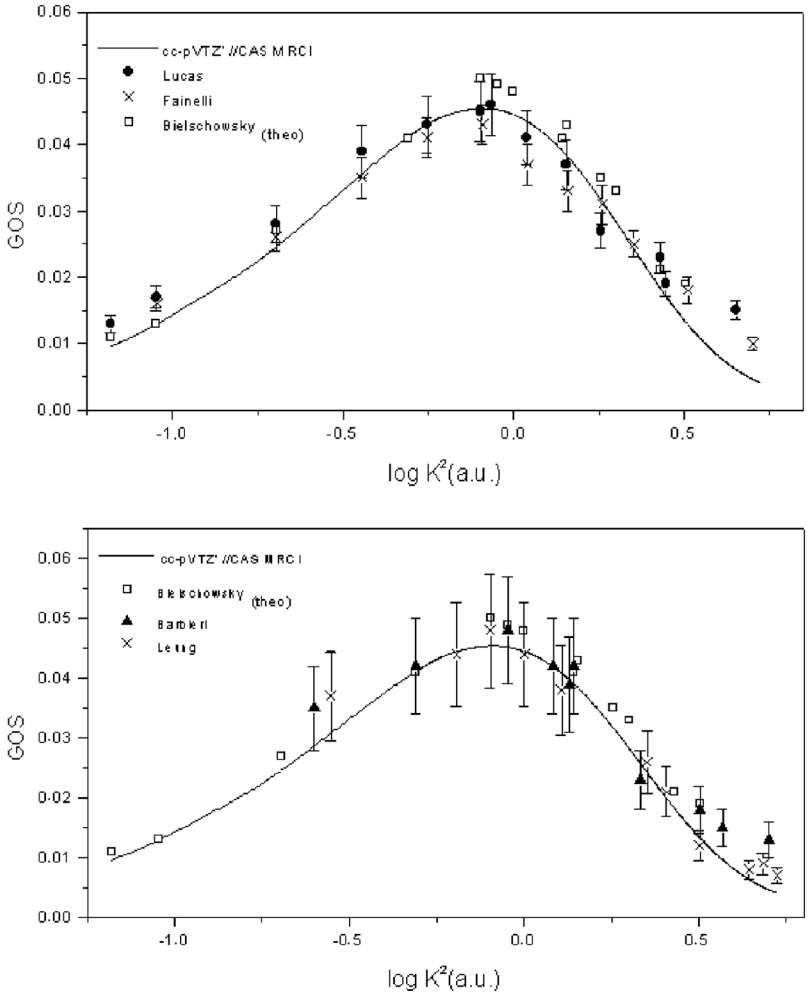

FIG. 2. Comparison between computed GOS profile computed at the cc-*p*VTZ′//CAS/MRCI level with nonorthogonal orbitals and available experimental data.

perimental results, separated in two panels for clarity reasons. Note the log scale in the square of the transferred momentum axis. In fact, as can be inferred from the GOS patterns shown in Fig. 1 using different wave functions, our most accurate GOS curve has the best agreement with experiment. The calculated transition energy at this level has also the best agreement with experiment, as can be seen in Table I.

In panels (a) and (b) our GOS curve is compared with the available experimental results excepting Wong *et al.* [8] as they are overestimated, as discussed later by the same group [12]. Previous theoretical results of one of us Ref. [1] are included in both panels as a past theoretical reference. The latter were the HF CI values including excitations up to quadruples.

The range of the transferred moment squared (K^2) in Fig. 2 goes up to 5.3a.u. In panel (a) it can be seen that our results show a good agreement with the experimental results of Lucas [10] and Fainelli [11], but diverges for large K^2 values. Our agreement at the maximum region is superior compared with previous theoretical results of one of us Ref. [1]. It is worth to notice that our GOS calculations using less correlated wave functions overestimates the maximum region values. The same conclusions can be drawn from the comparisons with other experimental results [panel (b)], the agreement with the most recent data of Leung [5] being quite good even for large K^2 values.

IV. CONCLUSION

Theoretical calculations of generalized oscillator strengths for the dipole-forbidden quadrupole-allowed of the Lyman-Birge-Hopfield of N_2 have been presented. For a long time our group has dedicated several efforts the interpretation of electron impact spectroscopy [1,3,4,23,24]. Recently, a more efficient computer code was developed for GOS and CI calculations, that was used in this work.

Several wave functions at the CAS and CI level and three different basis sets have been employed. We could clearly establish the following hierarchical sequence of wave functions: CAS, CAS CISD*, CAS CISD, CAS MRCI*, and CAS MRCI. All the CI calculations employed the full set of orbitals generated by the corresponding Gaussian basis set except the ones that have the label* that used a reduced active space composed of the first 20 orbitals. We have compared HF and CAS wave functions as a previous step before the MRCI calculations. It was verified the presence of differences between the respective GOS profiles, with the CAS MRCI GOS profile being slightly closer to the experiment than the HF MRCI one. Concerning the basis sets, it could be settled that the superiority of the Dunning correlation consistent basis sets as opposed to "hand-made" ones. Relaxation

effects were shown to play a considerable role in transition energies and GOS calculations. The GOS results obtained at the highest level, CAS MRCI//cc-*p*VTZ′, presented very good agreement with experimental results, including recent ones.

ACKNOWLEDGMENTS

The authors gratefully acknowledge the support of CNPq, FAPERJ, and CAPES, Brazilian agencies, for financial support.

[1] C. E. Bielschowsky, M. A. C. Nascimento, and E. Hollauer, Phys. Rev. A **42**, 5223 (1990).
[2] W. F. Chan, G. Cooper, R. N. S. Sodhi, and C. E. Brion, Chem. Phys. **170**, 81 (1993).
[3] I. Borges, Jr., G. Jalbert, and C. E. Bielschowsky, J. Phys. B **31**, 3703 (1998).
[4] I. Borges, Jr. and C. E. Bielschowsky, Phys. Rev. A **60**, 1226 (1999).
[5] K. T. Leung, J. Electron Spectrosc. Relat. Phenom. **100**, 237 (1999).
[6] Z. Chen and A. Z. Msezane, Phys. Rev. A **70**, 032714 (2004).
[7] A. Skerbele and E. N. Lassetre, J. Chem. Phys. **53**, 3806 (1970).
[8] J. S. Lee, T. C. Wong, and R. A. Bonham, J. Chem. Phys. **63**, 1643 (1975).
[9] N. Oda and T. Osawa, J. Phys. B **14**, L563 (1981).
[10] G. G. B. de Souza and C. A. Lucas, in *ICPEAC Book of Abstracts, Palo Alto*, edited by M. J. Coggiola, D. L. Heustis, and R. P. Saxon (North-Holland, Amsterdan, 1985), p. 252.
[11] E. Fainelli, R. Camilloni, G. Petrocelli, and G. Stefani, Nuovo Cimento D **9**, 33 (1987).
[12] R. S. Barbieri and R. A. Bonham, Phys. Rev. A **45**, 7929 (1992).
[13] A. Szabo and N. S. Ostlund, Chem. Phys. Lett. **17**, 163 (1972).
[14] S. Chung and C. C. Lin, Phys. Rev. A **6**, 988 (1972).
[15] M. Inokuti, Rev. Mod. Phys. **43**, 297 (1971).
[16] B. O. Roos, P. R. Taylor, and P. E. M. Siegbahn, Chem. Phys. **48**, 157 (1980).
[17] I. Borges, Jr., J. Phys. B **39**, 641 (2006).
[18] T. H. Dunning, J. Chem. Phys. **90**, 1007 (1989).
[19] C. W. Bauschlicher, J. Chem. Phys. **72**, 880 (1980).
[20] I. Borges, Jr., Chem. Phys. **328**, 284 (2006).
[21] T. Helgaker, T. A. Ruden, P. Jørgensen, J. Olsen, and W. Klopper, J. Phys. Org. Chem. **17**, 913 (2004).
[22] E. R. Davidson and A. A. Jarzecki, Chem. Phys. Lett. **285**, 155 (1998).
[23] E. Hollauer, M. L. Rocco, M. C. A. Lopes, and G. G. B. de Souza, J. Electron Spectrosc. Relat. Phenom. **104**, 31 (1999).
[24] G. G. B. de Souza, M. L. Rocco, H. Boechat-Roberty, C. A. Lucas, I. Borges, Jr., and E. Hollauer, J. Phys. B **34**, 1005 (2001).